Järvensivu, Mika; Saari, Kari; Jämsä-Jounela, Sirkka-Liisa

Intelligent control system of an industrial lime kiln process

Published in:
Control Engineering Practice

DOI:
10.1016/S0967-0661(01)00017-X

Published: 01/01/2001

Document Version
Publisher's PDF, also known as Version of record

Please cite the original version:
Järvensivu, M., Saari, K., & Jämsä-Jounela, S.-L. (2001). Intelligent control system of an industrial lime kiln process. *Control Engineering Practice*, *9*(6), 589-606. https://doi.org/10.1016/S0967-0661(01)00017-X

PERGAMON

Control Engineering Practice 9 (2001) 589–606

CONTROL ENGINEERING PRACTICE

www.elsevier.com/locate/conengprac

Intelligent control system of an industrial lime kiln process

M. Järvensivu[a,*], K. Saari[b], S.-L. Jämsä-Jounela[a]

[a]Helsinki University of Technology, P.O. Box 6100, FIN-02015 HUT, Finland
[b]UPM-Kymmene, P.O. Box 42, FIN-68601, Pietarsaari, Finland

Received 6 October 1999; accepted 20 October 2000

Abstract

In the face of strong competition, the pulp and paper industry is aiming at higher profitability through increased productivity and the reduction of costs. In addition, on the global scale the industry is facing increasing market demands for higher product quality, more specialty products and improved production flexibility and environmental protection. Consequently, extensive research is being conducted to improve existing processes. One alternative, which is gaining increasing attention within the industry, is the improved control of existing processes by means of intelligent systems. In this paper, an intelligent kiln control system is presented. In the system, neural network models are used in conjunction with advanced high-level controllers based on fuzzy logic principles and a novel linguistic equation approach. Finally, the testing results of the system are presented and discussed.

Keywords: Intelligent systems; Supervisory-level control; Rotary kiln; Energy consumption; Quality; Emissions

1. Introduction

The complex dynamics and multi-variable nature of the calcination process, with its non-linear reaction kinetics, long time delays and variable lime mud feed characteristics, make the lime kiln process inherently difficult to operate efficiently. During its operation, many interconnected variables must be considered and control actions must be designed to meet multiple and sometimes conflicting objects, and changing operating conditions. Furthermore, some of the measurements are unreliable, and the kiln characteristics may change during a long run. The lime kiln operation may also be upset by disturbances such as changes in the composition and/or properties of the lime mud. In addition, certain process variables must be maintained within predefined constraints in order to assure safe operation of the kiln process and for protecting the environment.

Supervisory-level control of the kiln process is thus in many respects, a demanding task. Lime kilns are therefore frequently one of the last areas in a pulp mill to be automated and most of the kilns have been and are still operated without a supervisory-level control system. In contrast, there are outstanding improvement potentials associated with the improved control. Firstly, energy efficiency can be improved considerably, and the benefits associated with a more stable lime quality can be significant when kiln control is improved (see Bailey & Willison, 1986 or Crowther, Blevins, & Burns 1987). The costs associated with repairing the refractory lining can also be reduced if the number of high temperature excursions is reduced, as reported in Dekkiche (1991) and in McIlwain (1992). Flue gas emissions can also be decreased when the occurrence of process upsets is eliminated, or at least reduced, by means of improved process control (Uronen & Leiviskä, 1989; Järvensivu, Kivivasara, & Saari, 1999).

The control of rotary kilns has been studied since the early 70s. The first applications were models based on the dynamics of the solids phase, the fundamental principles of heat transfer mechanisms, and the kinetics of drying, heating and calcining reactions. The developed models were used to estimate the temperature of solids, flue gas and refractory along the length of the kiln. These models, and many of the models since developed, have provided a useful insight into the rotary kiln process and also increased our understanding of the interactions and time delays inherent in the kiln process (see e.g. Brown & Rastogi, 1983 and Smith & Edwards, 1991).

* Corresponding author. Tel.: +358-9-451-3852; fax: +358-9-451-3854.
E-mail address: mika.jarvensivu@hut.fi (M. Järvensivu).

0967-0661/01/$ - see front matter
PII: S0967-0661(01)00017-X

Although phenomenological models have been relatively successful in simulating the operation of a rotary kiln very few, if any, of these models have been extended from the simulation stage to the control of an industrial scale kiln. The main reason for that have been the difficulties to achieve an adequately accurate model of the rotary kiln process. Therefore, the main emphasis turned to developing supervisory-level control systems based on empirical models, as described e.g. in Uronen and Aurasmaa (1979). The first commercial supervisory-level system for the lime kiln was developed on the basis of these studies and its first industrial applications appeared already at the end of the 1970s in a Finnish pulp mill (Sutinen, 1981). Other rotary kiln control systems based on the empirical models were also reported during the 1980's in the United States (see e.g. Bailey & Willison, 1985).

The first experiments in applying fuzzy logic to rotary kiln control were carried out at a cement plant in 1978, and the first lime kiln control system based on fuzzy logic was installed in a Swedish pulp mill in the following year (Ostergaard, 1993). Other industrial, fuzzy logic based kiln control applications have since been reported (Scheuer & Principato, 1995; Nilsson, 1997). The first rule-based expert system for kiln control was developed in 1982 and, since then, the system has been further developed as described in Haspel, Taylor, and Brooks (1991) and in Dekkiche (1991). Other rule-based systems for controlling rotary kilns have also been developed and reported (see e.g. Hall, 1993 and Hagemoen, 1993).

In addition to fuzzy logic and rule-based systems, rotary kiln applications based on the model predictive control approach have been reported in the literature during the 90s. Simulation results are described in Charos, Taylor, and Arkun (1991) and in Zanovello and Budman (1999), while the results of an industrial application can be found in Smith and Aggarwal (1998) and in Valiquette (1999). A neural network based system has also been tested for the control of the simulated kiln and also proposed for an industrial application, as reported in Ribeiro and Correia (1995). A rule-based kiln control system, in which neural networks are used to represent the rule set, has been reported in Yang, Yi, and Shouning (1997). Recently, a rotary kiln control system incorporating a predictive-adaptive controller to maintain the process close to the setpoints being generated by an expert system was described in Barreto (1997). In the same paper, neural networks in combination with the expert system were proposed as a potential candidate for future development.

To sum up, the state of the art in the rotary kiln control is that the systems based on the fuzzy logic and rule-based approach have already proven their applicability for controlling industrial kilns and systems combining various intelligent control and prediction techniques will be the future trend. In this paper, the structure and main functions of the supervisory-level control system of the lime kiln, which has been implemented at the Wisaforest pulp mill in western Finland, is presented. In the modular and hierarchically structured system, neural network models are used in conjunction with advanced high-level controllers based on fuzzy logic principles and a novel linguistic equation approach. Finally, the results obtained during the five-month testing period of the system are discussed and an assessment of the achieved benefits presented.

2. Process description

The causticizing process, which is a part of chemical recovery at the pulp mill as presented in Fig. 1, produces white liquor from green liquor. This process consumes lime, CaO, and produces lime mud, principally $CaCO_3$, as a by-product. The purpose of calcination is to convert the mud back into lime for reuse in the causticizing. The prime method used for calcination in the pulp industry is a rotary kiln. Conceptually, the lime kiln, which is a large cylindrical oven, can be divided into four process zones according to the temperature profile of the solids material and the flue gas in the kiln. These four zones are drying of the wet mud, heating of the mud powder up to the reaction temperature, calcining of calcium carbonate into calcium oxide, and agglomeration of the formed fine powder into granules. The endothermic calcining reaction (Eq. 1) starts at about 800°C, and the reaction heat required is 1.8 MJ/kg $CaCO_3$ decomposed.

$$CaCO_3(s) + \text{heat} \rightarrow CaO(s) + CO_2(g) \quad (1)$$

An overview of the lime kiln process at the Wisaforest pulp mill is presented in Fig. 2. The lime mud is first washed and then de-watered by means of two parallel vacuum drum filters. After the filters, the mud at about

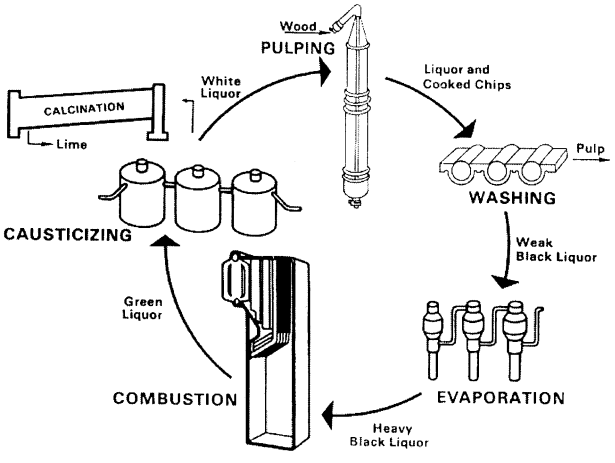

Fig. 1. Causticizing process as a part of the pulp mill chemical recovery circuit.

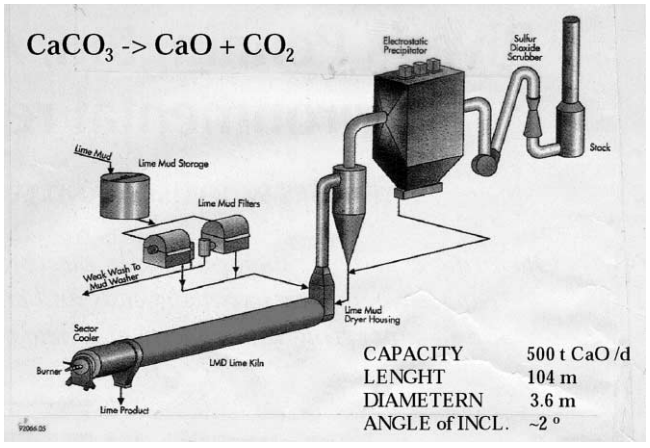

Fig. 2. Overview of the lime kiln process at the Wisaforest pulp mill.

75% dry solids is conveyed to a screw feeder, which distributes it into the flue gas duct. The flue gas then carries the mud into a cyclone, which is called the lime mud drier (LMD). Simultaneously, heat is transferred from the flue gas to the wet mud, which evaporates off the residual moisture. The dried and preheated mud powder is discharged from the bottom cone of the cyclone and fed into the cold-end of the kiln. After the LMD cyclone, the flue gas passes through an electrical precipitator and two-stage venture type wet scrubber. The dust, which is captured in the electrical precipitator, is fed back into the kiln together with the preheated mud. The mud powder then moves down the gradient of the kiln as a result of the inclination and rotation, and the burnt lime is discharged from the kiln through the product coolers located at the hot-end of the kiln. About 80% of the total heat energy input into the kiln is obtained by gasifying sawmill dust in a circulating fluidized bed gasifier and then, burning the generated gas in a burner installed at the hot-end of the kiln. Heavy fuel oil is only used as a secondary fuel. Primary combustion air, which is taken between the stationary hood and the product coolers, is forced into the kiln together with the fuel. Secondary combustion air is induced into the kiln by a low negative pressure maintained by an induced draught fan located after the electrical precipitator in the kiln exhaust system. The resulting counter-current flow of the hot combustion gases from the hot-end to the cold-end of the kiln distributes the heat energy along the length of the kiln.

3. Background and objectives of the project

The kiln process has been extensively studied at the Wisaforest mill since the beginning of the 90s. A kiln control system based on fuzzy logic was developed during 1993. Further details on the system, which was formulated on the basis of operator interviews and implemented in the DCS, can be found in Penttinen (1994) and in Ruotsalainen (1994). Encouraged by the promising results, the research was continued with the main emphasis on applying a novel linguistic-equation approach for fuzzy modeling and simulation of the kiln process (see e.g. Juuso, Ahola, & Leiviskä, 1996).

A field survey of the operation of the kiln process with special attention paid to the reduced sulfur emissions was carried out concurrently at the mill. The results of the survey showed, in addition to a considerable enhancement potential in the performance of the kiln process, that improved control is also a feasible means of reducing kiln emissions (Järvensivu, Kivivasara, & Saari, 1999). The research was then continued with the aim of developing, on the basis of the accumulated process knowledge, a supervisory-level control system for the kiln process. Preliminary results of the kiln control system are reported for e.g. in Sievola (1999), Järvensivu, Juuso, Sievola, Leiviskä, and Jämsä-Jounela (1999), and Järvensivu and Jämsä-Jounela (1999).

4. Overall structure of the kiln control system

The lime kiln control system at the Wisaforest pulp mill consists of in addition to basic instrumentation, on-line analyzers, a process automation system and an information system, an intelligent supervisory-level system, as illustrated in Fig. 3. The basic instrumentation of the kiln process includes for instance electromagnetic flow meters, radioactive density meters, pressure sensors, thermocouples and a pyrometer. On-line analyzers are used for measuring excess oxygen and sulfur dioxide of the flue gas and total reduced sulfur (TRS) emissions. The kiln instrumentation is presented in Fig. 4.

The automation system (ALCONT), which is a DCS supplied by Honeywell-Measurex, provides an interface to the basic instrumentation and the flue gas analyzers, and also carries out the handling of alarms, safety interlocks and logic sequences, as well as basic-level control

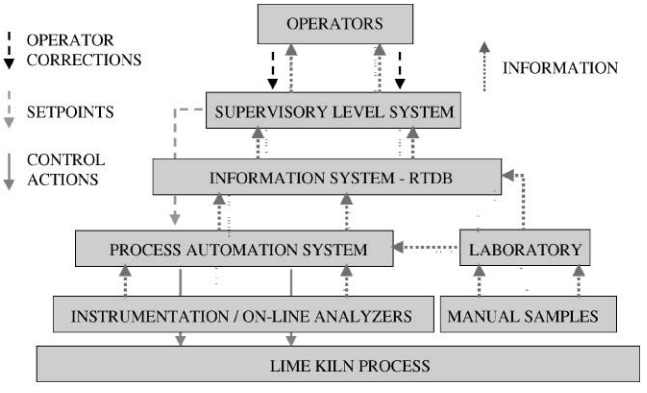

Fig. 3. Overall structure of the kiln control system.

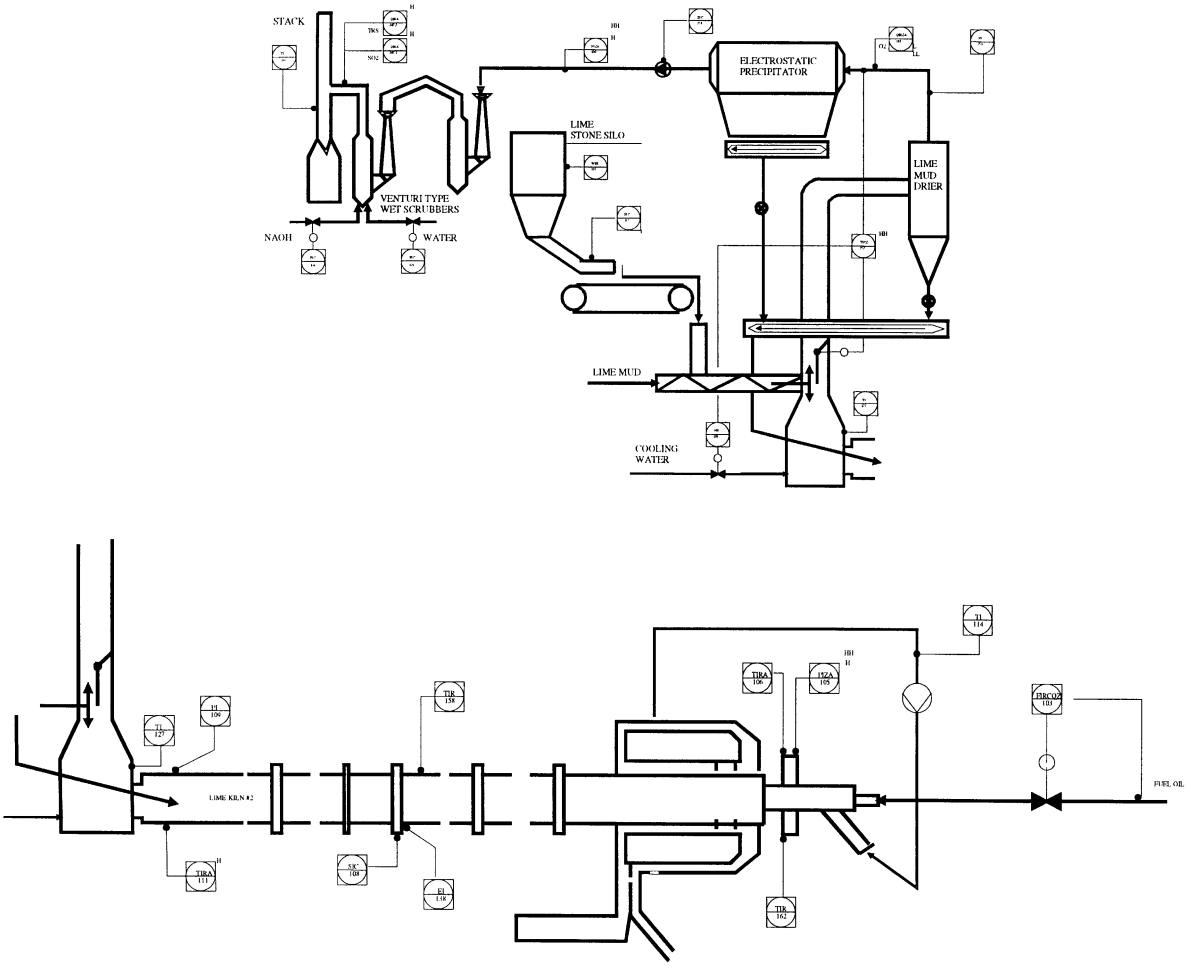

Fig. 4. Basic instrumentation of the kiln process.

loops. The information system, XIS supplied by Neles Automation, is used to collect all the kiln process measurements from the automation system, and it provides also access to the results of the laboratory analysis. The information system also performs the calculations of the average values at different time intervals, and archives both the current and historical data into the real time database (RTDB). The major measurements, the frequently performed laboratory analysis, and the most important basic-level control loops of the kiln process are listed in Tables 1 and 2, respectively.

The supervisory-level system is implemented using a Windows NT workstation and G2, which is an object-oriented environment for developing and deploying intelligent systems, from Gensym. The system is divided into hierarchically structured modules, as illustrated in Fig. 5. The lowest level of the system provides bi-directional interface to the low-level systems through a bridge to the RTDB of the information system. It also calculates the specific values required at a higher level in the application. The next level in the hierarchy has been designed to ensure stable operation of the kiln process. In practice, it is done by means of appropriate changes made in the setpoints (SPs) of the basic-level control loops, which are implemented in the DCS system. The purpose of the highest level in the hierarchy is to optimize the kiln process operation in respect to the lime quality, kiln

Table 1
Major measurements and laboratory analysis

On-line measurements	Laboratory analysis
Lime mud flow rate (l/s)	Lime mud feed
Lime mud density (kg/dm^3)	Dry solids content (%)
LMD temperature (°C)	Residual alkaline (%)
Cold-end temperature (°C)	Residual CaO (%)
Hot-end temperature (°C)[a]	
Burning zone temperature (°C)[b]	Burnt lime;
Cold-end pressure (mbar)	Residual $CaCO_3$ (%)
Kiln drive torque (%)	Causticizing efficiency (%)
Excess oxygen (%)	
TRS emissions (ppm)	

[a] Thermometer.
[b] Pyrometer.

energy efficiency and environmental protection by means of determining the optimum target values for the stabilizing-level controllers.

5. High-level control of the kiln process operation

5.1. Controlled, constraint and manipulated variables

In the kiln process at the Wisaforest pulp mill, as in all the other lime kiln processes as well, the primary output variables such as the residual $CaCO_3$ content and causticizing efficiency of the burnt lime, are not measured on-line. For instance, at the Wisaforest case the burnt lime is manually sampled with an 8 h time interval and the residual $CaCO_3$ content of the sample is analyzed with a delay time of about 2 h in the laboratory. The laboratory analysis is significantly delayed and therefore, impracticable from the control point of view. Therefore, measurable state variables with known correlation with the primary process outputs need to be chosen as controlled variables.

In the Wisaforest case, the excess oxygen content of the flue gas after the LMD cyclone, the temperature of the flue gas in the cold-end of the kiln and the hot-end temperature measured by means of a thermometer were selected as controlled variables. The excess oxygen and cold-end temperature are closely related with both the flue gas emissions and heat losses. Whereas, the hot-end temperature affects first and foremost the lime quality, but also the heat energy consumption. Besides the controlled variables the total reduced sulfur (TRS) emissions, LMD temperature and pressure in the cold-end of the kiln were selected as constraint variables. While, the draught fan speed and sawdust feed rate were selected as the manipulated variables of the control system due to a strong and predictable correlation with both the controlled and constraint variables. The rotational kiln speed was also selected as a manipulated variable, because it provides a mean for the control of the residence time of the solids material in the kiln. The controlled, constraint and manipulated variables are summarized in Table 3.

Table 2
Basic-level control loops

Controlled variables	Manipulated variables
Lime mud flow rate (l/s)	Feed pump speed (rpm)
Lime mud density (kg/dm^3)	Dilution valve position (%)
Draught fan speed (rpm)	Inverter (fan motor) (rpm)
Kiln rotational speed (rpm)	Inverter (kiln drive) (rpm)
Sawdust feed rate (%)	Inverter (feeder speed) (%)
Fuel oil flow rate (kg/s)	Valve position (%)

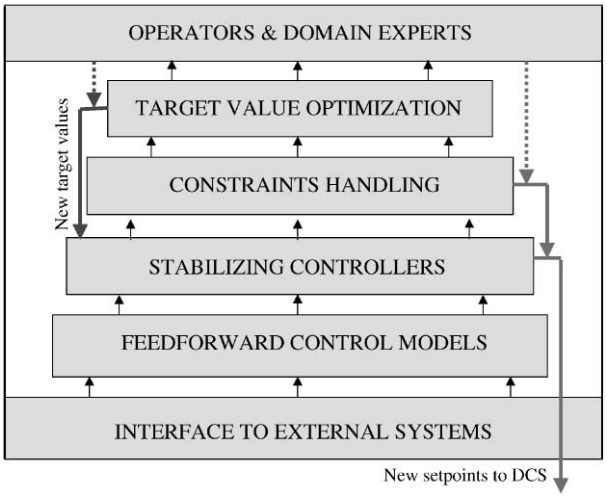

Fig. 5. Hierarchical structure of the supervisory-level control application.

5.2. High-level control modules

The high-level control of the kiln process is carried out by means of the inter-related modules of the feedforward control models, stabilizing controllers and constraints handling, as illustrated in Fig. 6.

The main purpose of the *feedforward control models* (FFMs) module is to take care of pending production rate change. The FFMs module manages production rate change by means of appropriate adjustments made in the setpoints of the basic-level control loops in the kiln process. The purpose of the *stabilizing controllers* (SCs) module is to provide adaptation after unmeasureable disturbances in the kiln process inputs or the process itself by means of small corrections in the SPs. On top of the SCs module, the *constraints handling* (CH) module is activated for protecting personnel, equipment and the environment when preset constraints are exceeded, e.g. in

Table 3
Controlled and manipulated variables of the high-level control system

Controlled variables	Constraint variables	Manipulated variables
Excess oxygen (%)	LMD temperature (°C)	Draught fan speed (rpm)
Cold-end temperature (°C)	Cold-end pressure (mbar)	Sawdust feed rate (%)
Hot-end temperature (°C)	TRS emissions (ppm)	Kiln rotational speed (rpm)

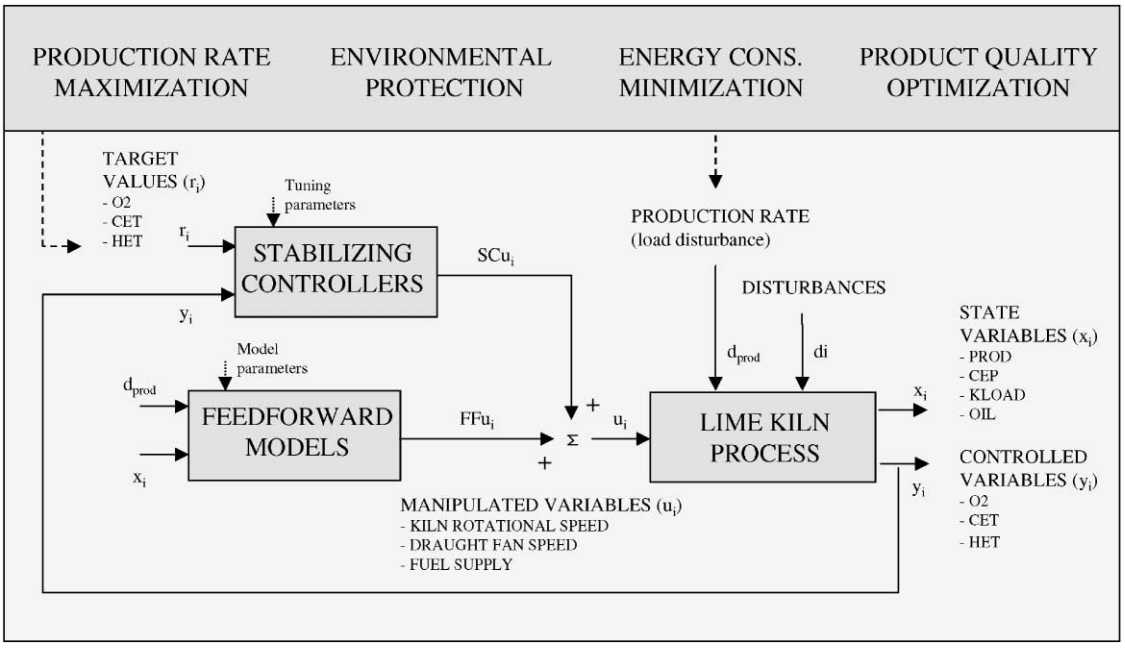

Fig. 6. Schematic presentation of the control structure.

the case of severe disturbances and/or abnormal process conditions. In addition, the CHs module is used to tackle large deviations from the target conditions by means of stepwise changes in the SPs.

The FFMs module relies on the predetermined relationships obtained from the large amount of process data collected at the Wisaforest mill. While, the SCs and CH modules rely on real-time inference of the state of the kiln process with respect to the target values that are determined at a highest level in the system as well as preset and dynamic constraints.

The new SPs for the draught fan speed (FAN), sawdust feed rate (DUST) and kiln rotational speed (KRPM) are determined based on the most recent outputs of the FFCs module, and the latest corrections made by means of the SCs module. Before enforcing the new setpoints into the DCS, they are however checked with respect to the acceptable range for the SPs in order to ensure safe operation of the kiln process in the case of instrument failures or other unexpected fault situations. The acceptable range is calculated by the system as a pipe around the FFu_i, as shown in Eqs. (2) and (3):

$$u_i^{hr}(k) = \mathrm{FF}u_i + \alpha_i \tag{2}$$

$$u_i^{lr}(k) = \mathrm{FF}u_i - \beta_i, \tag{3}$$

where u^{hr} and u^{lr} are the high and low boundaries, respectively. α_i and β_i are constants used to calculate the width of the range for acceptable SPs. The acceptable range is also limited by the preset low and high limits, u_i^{ll} and u_i^{hl}, respectively. The principle used in determining the SPs is also illustrated schematically in Fig. 7. The output of the FFMs module is shown in the figure as a non-linear curve in the middle of the range for the acceptable SP. Whereas, the latest value of the SCu_i, and CHu_i, which are add to (or subtract from) the FFu_i determine the actual value of the setpoint. Table 4 gives the tuning-parameter values used for the constants (α_i and β_i), and the high and low limits (u_i^{hl} and u_i^{ll}) used in the current version of the system, while, each of the modules is described in more detail below.

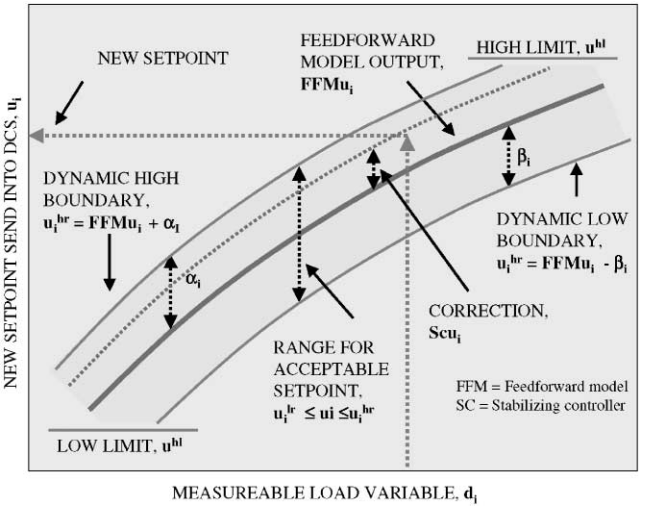

Fig. 7. Principle used in determining the new SPs for basic level control loops.

Table 4
Tuning-parameter values used for determining the acceptable range for the SPs

	u^{lr}	U^{hr}	α	β
Draught fan speed (rpm)	700	960	30	30
Sawdust feed rate (%)	25.0	80.0	10	10
Kiln rotational speed (rpm)	1.40	1.70	0.03	0.03

Table 5
Tuning parameter values of the model applied for FFC of the kiln rotational speed

FFC; kiln rotational speed				
A	b_1	b_2	m	N
1.16	0.012	−0.023	15	18

5.2.1. Feedforward control models

The model used for the feedforward control (FFC) of the *kiln rotational speed* is a multiple linear regression (MLR) model, as shown in Eq. (4),

$$FFu_{KRPM}(k) = f_{MLR}(\bar{d}_{prod}, \bar{x}_{CEP}) = a + b_1 \sum_{j=k-m}^{k-1} \frac{d_{PROD}(j)}{m} + b_2 \sum_{j=k-n}^{k-1} \frac{x_{CEP}(j)}{n}, \quad (4)$$

where m and n stand for the number of 10 min average values used to calculate the moving averages of the production rate (d_{PROD}) and the cold-end pressure (x_{CEP}), respectively. Table 5 presents tuning parameter values used for the intercept, the regression coefficient and determining the number of measurement used in the moving average calculation. The model complies with the relationship between the production rate and kiln rotational speed obtained from the kiln manufacturer, who recommends that the rotation speed is increased along with increasing production rate in order to maintain a constant filling rate in the kiln. In addition, the model takes into account the cold-end pressure, which is used to indirectly indicate undesired ring formation in the cold-end of the kiln. An increase in the kiln rotational speed when the cold-end pressure is decreased is used to prevent further ring formation and to promote removal of the existing ring.

The models used for the FFC of the *draught fan speed* and *sawdust feed rate* are backpropagation neural network (NN) models. The NN models with linear transfer functions in the input and output layer, and sigmoidal transfer functions in the hidden layer, are applied due to the non-linear relationships obtained between the variables. NN models with two input variables, single output variable, and one hidden layer and as few as possible hidden nodes are, however, applied. Models with a greater number of hidden nodes were also tested and those gave smaller training and even testing errors than the applied models. Despite the smaller errors, these models generated unexpected outputs with certain combinations of the input pairs, for the reason that those larger networks tended to learn also uncharacteristic correlation found in the data. In this case, robustness with respect to the noisy process data is more important than close correlation with the training data in order to provide models with a predictable behavior.

The inputs of the model used for the FFC of the *draught fan speed* are the 150 min moving average of the production rate and the 180 min moving average of the cold-end pressure. The inputs and corresponding scaling factors, as well as configurations of the model is presented in Table 6. Fig. 8 shows the output of the model as a function of the production rate, which has a dominant influence on the output. The draught fan speed is increased to ensure a proper flow of the combustion air into the kiln, i.e. an appropriate level of the excess oxygen in the flue gas, when the production rate is raised, and vice versa. The other input in the model, the cold-end pressure, is used to compensate the restrictive influence of the existing ring on the flue gas flow, and hence also on heat transfer from the burning zone to the cold-end of the kiln.

Two separate NN models, described in more detail in Tables 7 and 8, are applied for FFC of the *sawdust feed rate* depending on the rate of heavy fuel oil burning, which is set manually at a level of between 0.1 kg/s and 0.3 kg/s when it is burned. The first model is used when sawdust is burned alone, and the other model when heavy fuel oil is burned as a secondary fuel in addition to sawdust. In both cases, the sawdust feed rate is altered in accordance with the 150 min moving average of the production rate. The first model also takes into account the 180 min moving average of the torque (load) of the kiln drive, which is an indirect indication of the amount of solids in the kiln. This is done in order to provide sufficient heat energy to the kiln for heating the solids up to the reaction temperature, and for calcining the calcium carbonate into calcium oxide, while ensuring that the lime is not over-burned. In the other model, the 10 min moving average of the flow rate of fuel oil is used as a second input in order to maintain the total heat energy input into the kiln despite the changes made to the fuel oil flow rate. Fig. 8 shows the output of the model as a function of the production rate, which has a dominant influence on the output.

In the above-described FFC models, which are executed at 10 min scan intervals, moving averages of the input variables can be applied to avoid fluctuation of the model outputs in the case of short-term disturbances in

Table 6
The model applied for FFC of the draught fan speed[a]

FFC; draught fan speed		
TRAINING DATA	1875 8 h average values	
	Range	Scaling
INPUTS	Minimum/maximum	Additive/multiplicative
Lime mud feed rate	20.0 t/h	− 20.828
(150 min average)	37.0 /h	0.062
Cold-end pressure	− 3.0 mbar	2.993
(180 min average)	0 mbar	0.314
OUTPUT		
New SP for draught	700 rpm	− 702.652
fan speed	980 rpm	0.004
NN MODEL	Type/size/transfer function	Type/size/transfer function
	Bnp/2, 1, 1/L, S, L	Bnp/2, 1, 1/L, S, L
	Weights	Weights
	0.215246	1 1 1
	− 0.824	2 1 1
	0.752336	3 1 1
	− 1.77358	1 1 2
	0.774167	2 1 2
	Rmse	0.156

[a] Bnp = Backpropagation neural network model.
X, X, X = Input, hidden and output layer nodes, respectively.
L = Linear transfer function, S = Sigmoidal transfer function.

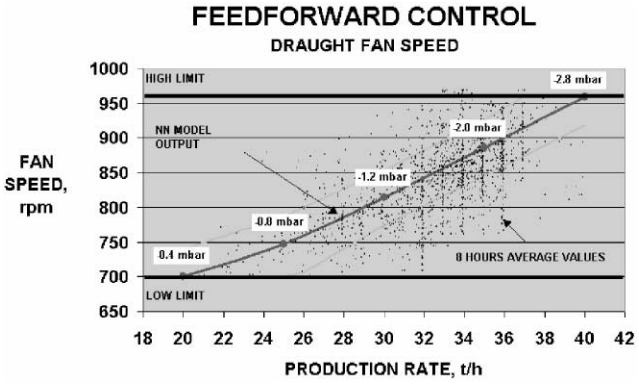

Fig. 8. Output of the FF control model for the draught fan speed as a function of the production rate.

the input variables. In addition, by using appropriate moving averages of the input variables straightforward steady-state models can approximate dynamic behavior of the process during gradual changes such as a pending production rate change (note: fast and unexpected changes occurring in the process are handled by means of the stabilizing controllers and/or constraint problem handling module). The width of the time windows applied for the input variables in the models were selected based on the domain knowledge of the applicable process delays and performed time series analysis of the collected process data.

5.2.2. Stabilizing controllers and constraints handling

The *draught fan speed* is corrected at 10 min scan intervals on the basis of the excess oxygen content of the flue gas and the temperature profile along the length of the kiln, by means of a SC based on fuzzy logic principles. The actual correction is a weighed average of the corrections determined to bring the excess oxygen content as well as the cold- and hot-end temperatures closer to the target values. The fuzzy logic approach is applied because an appropriate correction to the draught fan speed is often a compromise between three conflicting corrections required to bring these three variables to their target values. An increase in the draught fan speed is used to increase the excess oxygen, raise the cold-end temperature and lower the hot-end temperature, and vice versa. Fig. 9 presents, as an example, the correction on the draught fan speed as a function of the error in the excess oxygen.

In addition, structured natural language rules together with procedural reasoning are used to check the LMD temperature each time a new measurement is obtained. If it is below the preset or dynamic limit then the draught fan speed is increased by the constraint handling (CH) module. Reasonable large step changes (about 5–10 times bigger than corrections made by means of the SC per one cycle) are used in order to eliminate the risk of increased emissions of hydrogen sulfide, and also to avoid the formation of acid condensates in the flue gas channel, both of which are formed due to the too low temperature during lime mud drying. The CH module is also used to

Table 7
The model applied for FFC of the sawdust feed rate when only sawdust is burned

FFC; sawdust feed rate		
TRAINING DATA	3029 1 h average values	
	Range	Scaling
INPUTS	Minimum/maximum	Additive/multiplicative
Lime mud feed rate	22.0 t/h	− 23.247
(150-minute average)	39.0 t/h	0.064
Kiln load	50.0%	− 52.816
(180-minute average)	85.0%	0.035
OUTPUT		
New SP for sawdust feed rate	35.0%	− 38.357
	80.0%	0.027
NN MODEL	Type/size/transfer function	Type/size/transfer function
	Bnp/2, 2, 1/L, S, L	Bnp/2, 2, 1/L, S, L
	Weights	Weights
	− 1.14375	1 1 1
	− 4.24697	1 2 1
	− 0.371727	2 1 1
	− 4.48297	2 2 1
	1.37113	3 1 1
	1.05292	3 2 1
	− 0.498007	1 1 2
	− 1.69875	2 1 2
	2.16238	3 1 2
	Rmse	0.168

Table 8
The model applied for FFC of the sawdust feed rate when heavy fuel oil is burned besides sawdust[a]

FFC; sawdust feed rate		
TRAINING DATA	3029 1 h average values	
	Range	Scaling
INPUTS	Minimum/maximum	Additive/multiplicative
Lime mud feed rate	20.0 t/h	− 20.417
(150 min average)	38.0 t/h	0.057
Heavy fuel oil	0.05 kg/s	− 0.071
(10 min average)	0.30 kg/s	4.367
OUTPUT		
New SP for sawdust	35.0%	− 38.357
feed rate	80.0%	0.027
NN MODEL	Type/size/transfer function	Type/size/transfer function
	Bnp/2, 1, 1/L, S, L	Bnp/2, 1, 1/L, S, L
	Weights	Weights
	− 2.24931	1 1 1
	2.04969	2 1 1
	− 2.44022	3 1 1
	0.594602	1 1 2
	0.823518	2 1 2
	Rmse	0.151

[a] BnP = Backpropagation neural network model.
X, X, X = Input, hidden and ouput layer nodes, respectively.
L = Linear transfer function, S = Sigmoidal transfer function.

increase the draught fan speed if the excess oxygen level is already low while, at the same time, the fuel supply into the kiln is increased either by the system or manually by the operator.

Correspondingly, the *sawdust feed rate* is corrected at 5 min scan intervals in order to maintain the cold- and especially hot-end temperatures at their target values. The small corrections to the SP of the sawdust feed rate

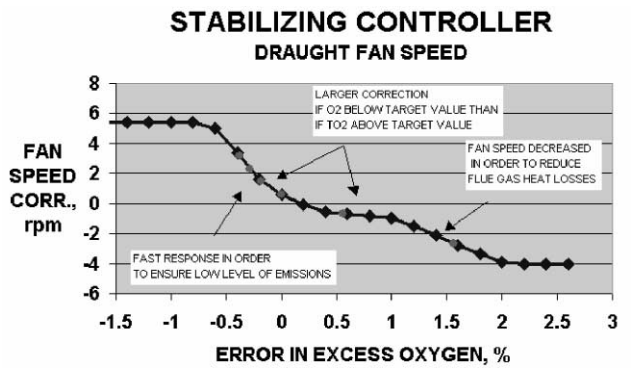

Fig. 9. Correction on the draught fan speed as a function of the error in the excess oxygen.

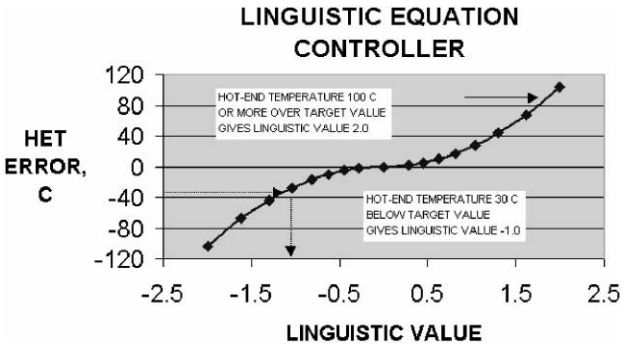

Fig. 10. Non-linear membership definition for the error in the hot-end temperature (HET).

are determined by means of a SC based on a novel PI-type linguistic equation (LE) controller providing enhanced features for handling non-linearity and disturbances, as well as for managing changes in the operating conditions.

The basic LE controller applied to determine appropriate correction to the sawdust feed rate is expressed as follows

$$\Delta \mathrm{SC}u_{\mathrm{DUST}}(k) = [f_{\mathrm{LE}}(e_{\mathrm{CET}}, \Delta e_{\mathrm{CET}}) + f_{\mathrm{LE}}(e_{\mathrm{HOT}}, \Delta e_{\mathrm{HOT}})], \quad (5)$$

where e_{CET}, e_{HET}, are the most recent error in the cold-, and hot-end temperature, respectively. While, Δe_{CET}, and Δe_{HET} stand for the change in the cold- and hot-end temperature during the last five minutes, respectively. Fig. 10 shows the non-linear membership definition for the error in the hot-end temperature as an example of the relationships between the real values and the linguistic values applied in the LE controller. While, Table 9 summarizes values of parameters a_i, b_i and c_i used to convert real values to linguistic values and vice versa.

Besides the basic LE controller, the braking action is automatically activated if the error in the cold- or hot-end temperature exceeds a certain value. Large errors occur from time to time especially in the hot-end temperature due to rapid changes in the heat energy content of the sawdust fed into the gasifier. The controller returns back to normal operation when the fast trend in the controlled variable is removed.

Changes in the operating conditions are taken into account by means of the WP equation. For instance, the corrections of the sawdust feed rate is at their largest when the production rate are high, and vice versa, because at a high production rate larger control actions are required to correct the same deviation as at a low production rate. In addition, the consumption of burning air in the sawdust gasifier, which correlates with the sawdust quality (SDQ), is used for scaling the corrections. Smaller corrections are made with high-quality sawdust than with low-quality sawdust. Scaling the determined corrections on the basis of the WP and SDQ, provides a certain level of adaptivity and hence, enables the single LE controller to be tuned for different operating conditions. In the case of a large deviation in the hot-end temperature, or fast changes in SDQ, the CH module is however activated for making stepwise correction to the sawdust feed rate in order to avoid extensive temperature excursions.

A PI-type LE controller is represented by a single linguistic equation as follows:

$$\Delta u = e + \Delta e, \quad (6)$$

where e is the linguistic value (LV) of the error, Δe is the LV of the derivative of the error and Δu is the LV of the change of the control variable. Eq. (6) is a special case of the matrix equation $AX = 0$ with the interaction matrix $A = [1\,1\,-1]$, which describe the direction of the interaction between variables, and linguistic variables defined as $X = [e\ \ \Delta e\ \ \Delta u]^{\mathrm{T}}$. In the LE approach non-linearity is handled by means of membership definitions, which correspond to membership functions used in conventional fuzzy logic controllers. Eq. (7) is used to convert real values (RVs) to linguistic values, while Eq. (8) is applied for re-converting LVs back to RVs.

$$LV_i = \begin{cases} 2 \text{ if } LV_i \geqslant 2, \\ \dfrac{-b_i + \sqrt{b_i^2 - 4a_i c_i}}{2a_i}, \\ -2 \text{ if } LV_i \leqslant -2, \end{cases} \quad (7)$$

$$RV_i = a_i LV_i^2 + b_i LV_i + c_i. \quad (8)$$

Changes in the operating conditions are taken into account by means of the working point (WP) equation. WP equation is used to scale the control surface of the basic LE controller by modifying the membership definitions for the change of control variable (Δu) according to

Table 9
Summary of tuning parameters values used to convert real values to linguistic values and vice versa[a]

SC; sawdust feed rate					
	a_i		b_i		c_i
	$c_i < 0$	$c_i > 0$	$c_i < 0$	$c_i > 0$	
HET					
e	− 26	26	0	0	RV_e
Δe	− 2.5	2.5	0	0	$RV_{\Delta e}$
Ie	− 5	5	5	5	RV_{Ie}
CET					
e	− 20	20	0	0	RV_e
Δe	− 7	7	0	0	$RV_{\Delta e}$
Ie	− 15.0	15.0	15.0	15.0	RV_{Ie}
DUST					
Δu	0.2	− 0.2	0	0	$LV_{\Delta u}$

[a]RV = real value of the variable, LV = linguistic value of the variable.

the operating conditions of the process, i.e. by making the control surface either flatter or steeper. The use of WP for scaling the output extends the basic LE controller to adaptive controller. In addition, the LE controller comprise so called predictive braking action, which emphasizes the influence of the change in the error, and correspondingly diminishes the influence of the error when the controlled variable approaches the target after a large initial error. Braking action, which corresponds to predictive switching control, reduces the risk for common problems such as oscillation and large overshoot after considerable disturbances. Above-described features, i.e. adaptation based on the WP and predictive braking action, are fully integrated in the basic LE controller, which ensure smooth operation of the LE controller over a large operational area (Juuso, Balsa, & Valenzuela 1998; Juuso, 1999).

6. Optimization of the kiln process operation

The improved stability of the process obtained by the high-level control modules allows operation of the kiln process closer to the constraints, and therefore closer to the optimum. In order to realize the benefits of the reduced variability, the target values of the controlled variables need to be shifted closer to the constraints. Control of the process within a narrowed safety margin, in the presence of unmeasurable changes in the process, necessitates additional supervision and corresponding high-level adjustments to the target values for fulfilling the objectives set on lime quality and energy efficiency as well as the limit set on emissions. The adjustments required to maintain the process close to the optimal state are computed by means of the target value module on the basis of the kiln operating conditions.

The target value for the *hot-end temperature* is determined by means of the NN model, which was developed on the basis of the process data. The model takes into account the 150 min moving average of the production rate, and the load of the kiln drive as well as the 10 min average value of the heavy fuel oil flow rate. The inputs and corresponding scaling factors, as well as configurations of the model is presented in Table 10.

While, Fig. 11 shows how the target value is increased in order to maintain the lime quality within the optimum range when the production rate or the torque of the kiln drive increases, and vice versa. The figure also illustrates the influence of heavy fuel oil burning on the calculated target value. The burning of heavy fuel oil affects the shape and length of the flame, and the proportion of cold secondary burning air also increases. As a result, the burning of heavy fuel oil has an influence on the range of the hot-end temperature readings, and hence, the target also needs to be adjusted.

The target value for the *cold-end temperature* is adjusted on the basis of the 150 min, moving average of the production rate, the LMD temperature, which correlates with the moisture content of the lime mud, and the cold-end pressure by means of an NN model. The model is used for calculating the adjustments needed to maintain the heat content of the flue gas at a proper level for drying and heating up the wet lime mud fed into the kiln. The target value is however lowered if the LMD temperature is high enough and increased accordingly when the LMD temperature decreases below the preset limit. The target value for the *excess oxygen content of the flue gas* is adjusted on the basis of the 120 min, moving average of the total reduced sulfur emission, which is not influenced by the rate of air infiltration before the measurement point. If the emissions are low enough, the target value is lowered with small steps in order to keep the heat losses caused by the hot flue gases leaving the kiln at the lowest

Table 10
The model applied in the calculation of the target value for the hot-end temperature[a]

TVC; hot-end temperature		
TRAINING DATA	5584 1 h average values	
	Range	Scaling
INPUTS	Minimum/maximum	Additive/multiplicative
Fuel oil flow rate	0.0 kg/s	0
(10 min average)	0.8 kg/s	1.25
Lime mud feed rate	20.0 t/h	− 20.26
(150 min average)	38.0 t/h	0.056
Kiln drive load	50.0%	− 50.069
(150 min average)	80.0%	0.033
OUTPUT		
New target value for hot-end temperature	470°C	− 470.547
	700°C	0.004
NN MODEL	Type/size/transfer function	Type/size/transfer function
	Bnp/3, 1, 1/L, S, L	Bnp/3, 1, 1/L, S, L
	Weights	Weights
	0.592933	1 1 1
	− 0.25561	2 1 1
	− 0.13548	3 1 1
	− 0.64359	4 1 1
	− 1.7144	1 1 2
	− 0.01051	2 1 2
	Rmse	0.112

[a] Bnp = Backpropagation neural network model.
X, X, X = Input, hidden and output layer nodes, respectively.
L = Linear transfer function, S = Sigmoidal transfer function.

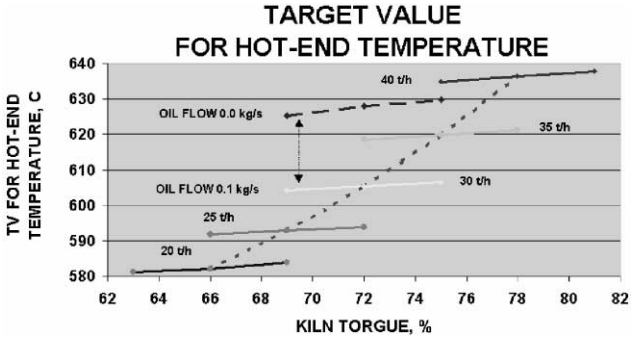

Fig. 11. Target value of the hot-end temperature as a function of the torque of the kiln drive.

possible level. In the opposite case, the target value is increased in order to avoid exceeding the limit if the emissions start to rise.

7. Results

7.1. Average runtime of the system

The supervisory-level system was connected on-line at the Wisaforest mill for first time at the end of February, 1998. The third version of the system, which is described in this paper, has been in operation since the beginning of February, 1999. The average runtime[1] of the system between March 1998 and June 1999 is shown in Fig. 12 on a monthly average basis. The average runtime in the closed loop mode was about 45% between March 1998 and January 1999 during the incremental development of the system. While, the average runtime in the closed loop mode has been over 85%, between February 1999 and June 1999 during the five-month testing period of the system. During the testing period, the system was entirely supervised by the operators, and reached a relatively high level of utilization of the system, which justifies the system acceptance by the operators.

7.2. Dynamic performance of the system

The dynamic performance of the system was verified based on the data collected during the continuous four-day runtime span at the beginning of April 1999. Fig. 13 presents the production rate (lower chart), and the hot-end temperature and excess oxygen (upper chart), i.e. the controlled variables, at the one-hour average level. Both

[1] The average runtime is calculated as the mean time of the draught fan speed, the sawdust feed rate and the rotational kiln speed control loops in the closed loop mode divided by the time that the kiln process has been in operation and the sawdust has been burned alone or together with heavy fuel oil.

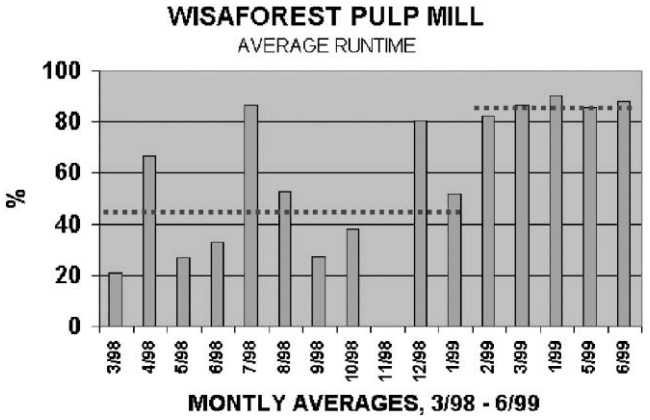

Fig. 12. Average runtime of the system between March 1998 and June 1999.

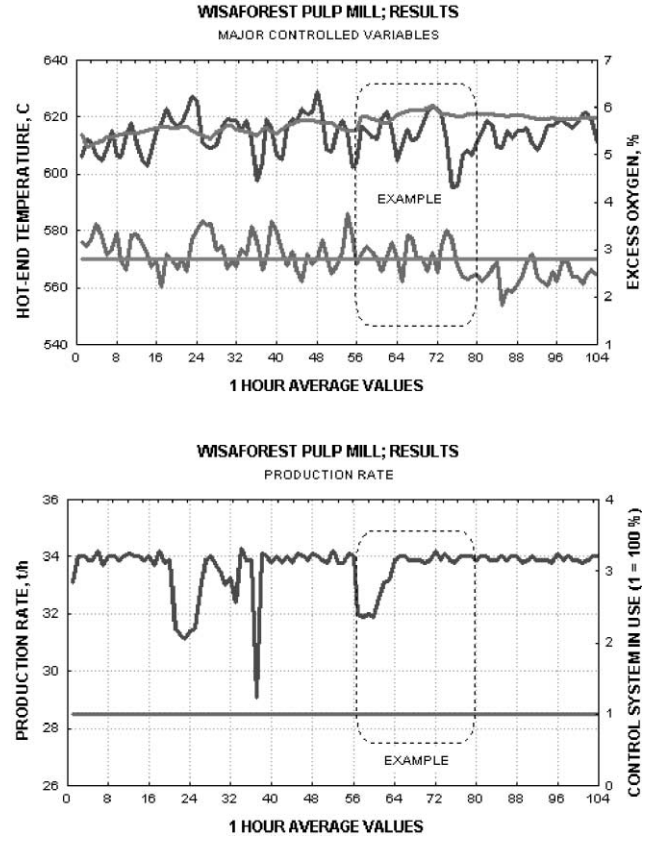

Fig. 13. Major controlled variables (above) and the production rate (below) during the continuous four-day runtime span of the control system.

controlled variables have been maintained relatively close to their target values despite large changes carried out on the production rate during the examined period, which demonstrates the ability of the system to track the target values of the controlled variables even in the face of considerable load disturbances.

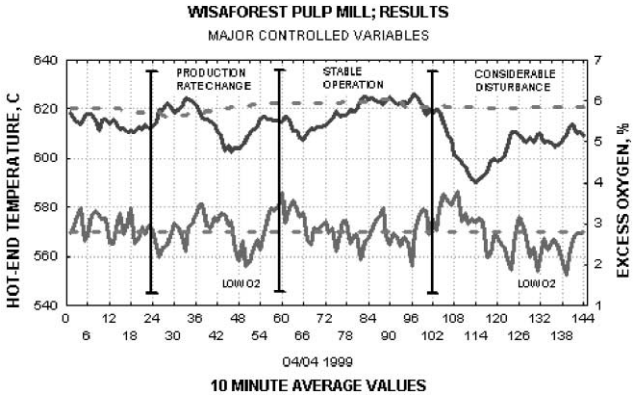

Fig. 14. Hot-end temperature and excess oxygen during the 24 h test-period.

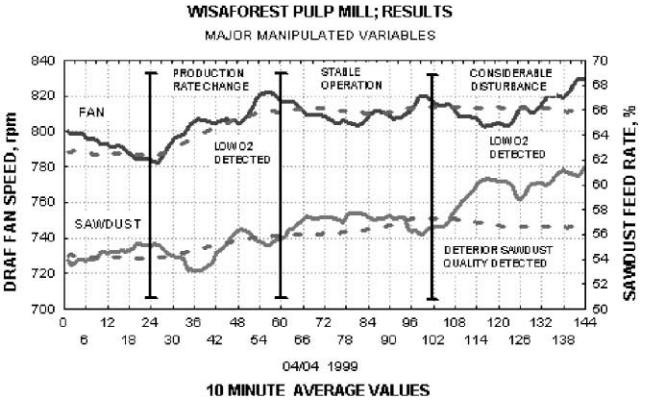

Fig. 15. Draught fan speed and sawdust feed rate during the 24 h test-period.

A 24 h period, which is marked with dashed line in Fig. 13, was selected for further analysis. The period includes intentionally, at first, a production rate change, and then an extended period of the kiln operation at the constant production rate. The hot-end temperature and excess oxygen at 10 min average level during the 24 h period are presented in Fig. 14. The figure shows that excess oxygen has been maintained between 1.8% and 3.8%, which is an appropriate range for the excess oxygen from the energy efficiency and environment protection points of view. Fig. 14 shows also that the hot-end temperature has been maintained relatively stable during the pending production rate change (the first section of the figure). The temperature has then successfully been stabilized at the target level shortly after the kiln process has reached a constant production rate, as illustrated in the second section of the figure.

The draught fan speed and sawdust feed rate during the same 24 h period are presented in Fig. 15. The continuous lines in the figure represent the actual values of the setpoints, while the dashed lines stand for the output

values of the feedforward module. Consequently, the difference between the continuous and dashed line corresponds to the correction made by the stabilizing controller, and/or constraints handling module. The first section of Fig. 15 shows that relatively large adjustments have been carried out by means of the feedforward module to compensate the influence of the production rate change. The dashed lines, i.e. the output values of the feedforward models, have however been leveled out, and only small corrections have then been carried out by the stabilizing controllers to maintain the target values when the kiln process has been operated at the constant production rate.

The examined 24 h period includes also a period of an exceptional fast decline in the temperature, shown at the beginning of the third section in Fig. 14. The fast decline (about 30°C in less than 2 h) was the consequence of a considerable disturbance in the heat energy input to the kiln caused either due to a decrease in the actual sawdust feed rate or a deterioration in the sawdust quality. The system responded on the decline of the temperature by an immediate and relative large increase in the sawdust feed rate and a gradual decrease in the draught fan speed, as illustrated in Fig. 15. As a result, the system was able to prevent the further decline of the temperature, and subsequently to bring the temperature back to an appropriate range. The fast response and especially the success in leveling out the temperature after the excursion demonstrates effective disturbance rejection capabilities of the system. Fig. 15 illustrates also two examples of corrections made based on the detection of the low level of the excess oxygen. These stepwise corrections on the draught fan speed, which were carried out by the constraint-handling module in order to prevent consequential total reduced sulfur emissions in the case of further decrease in the excess oxygen, exemplify the system capability to handle also constraint problems.

7.3. Statistical analysis of the obtained results

The evaluation of the operational results was carried out by means of the statistical analysis of the data collected during the manual operation, between December 1996 and February 1998 and the corresponding data obtained during the five-month testing period of the system. First, the large amount of raw data was pre-processed. During pre-processing the erroneous measurements and invalid data that were collected during abnormal situations were systematically rejected. Comprehensive statistical analysis was then performed in parallel on the data collected during the manual operation and the testing period (see Table 11). The statistics concerning excess oxygen and the hot-end temperature are discussed in more detail below.

The mean value of the *excess oxygen* content of the flue gas measured after the LMD cyclone was 3.9% during manual operation, and the lower and upper quartiles (i.e. 25th and 75th percentile) were 3.2% and 4.5%, respectively. During the testing period of the system, the mean value of the excess oxygen was 3.3%, and the lower and upper quartiles were 2.8% and 3.8%, respectively. According to the statistics, the mean value has been reduced by about 15% and the quartile range has been decreased by more than 20% (see Fig. 16). The mean value of the hot-end temperature measured by means of a thermometer was 645°C during manual operation, and the lower and upper quartiles were 627°C and 665°C, respectively, when sawdust has been used as a primary fuel.[2] During the testing period, the mean value was 608°C and the lower and upper quartiles were 600°C and 620°C, respectively. The mean value has been reduced by nearly 40°C, and the quartile range and the standard deviation have declined nearly 50% and more than 30%, respectively (see Fig. 17).

7.4. Assessment of benefits

The major quantifiable benefit in an economical sense was a noteworthy reduction in the *heat energy consumption*. During the testing period between February 1999 and June 1999, the mean of the specific heat energy consumption (5.5 GJ/t_{CaO}) was nearly 7% lower than the respective value during the manual operation (5.9 GJ/t_{CaO}), when data collected during similar operating conditions were compared. A decrease in the heat energy consumption is associated with a decrease in the excess of burning air (see Fig. 16 and Table 11), i.e. the energy unnecessarily used to heat up cold burning air. It is also related to a reduction in both the cold- and hot-end as well as burn lime temperature (see Fig. 17 and Table 6), which indicates a subsequent reduction in the heat losses caused by radiation from the kiln shell into the surroundings.

The decline in the energy consumption has been considerable over the entire production rate range and the decline has been greatest at low production rates, see Fig. 18.[3] Furthermore, if we assume an average production rate of 32 t/h, and the quantified reduction in the mean of the energy consumption is utilized, the savings in energy account for about one million Finnish marks per annum.

[2] Temperature readings below about 580°C arise when oil is burned and there is a subsequent increase in the amount of cold burning air flowing past the thermometer that is mounted on the front-wall of kiln. This lowers the range of the temperature readings by nearly 100°C compared to the situation when pure sawdust is burned.

[3] Fig. 18 illustrates the heat energy consumption as a function of the production rate during manual operation and the testing period after the preprocessed data had first been classified into four groups according to the production rate (i.e. 22–26, 26–30, 30–34, and 34–38 t/h) and the mean in each group calculated.

Table 11
Summary of the descriptive statistics

		Mean	Lower/upper quartile		Std. Dev.
Production (t/h)	MAN	32.5	31.0	34.9	3.2
	TEST	32.7	31.8	34.0	2.8
Draught fan (rm)	MAN	839	797	879	55.2
	TEST	801	770	830	45.2
Heat energy	MAN	5.9	5.4	6.2	0.7
(GJ/tCaO)	TEST	5.5	5.1	5.8	0.5
Fuel oil (Kg/s)	MAN	0.18	0.00	0.17	0.22
	TEST	0.10	0.00	0.00	0.23
Kiln speed (rm)	MAN	1.57	1.52	1.60	0.06
	TEST	1.62	1.60	1.66	0.07
LMD temp. (°C)	MAN	247	227	267	25.5
	TEST	247	230	263	23.9
Cold-end temp. (°C)	MAN	635	621	648	19.1
	TEST	616	603	630	23.9
Hot-end temp. (°C)[a]	MAN	628	609	661	46.3
	TEST	599	590	619	31.1
Hot-end temp. (°C)[b]	MAN	645	627	665	26.5
	TEST	608	600	620	17.8
Burning temp. (°C)	MAN	1063	996	1139	103
	TEST	1028	100 2	1076	74
Excess O_2 (%)	MAN	3.9	3.2	4.5	1.0
	TEST	3.3	2.8	3.8	0.9
Residual $CaCO_3$ (%)	MAN	2.6	1.8	3.4	1.2
	TEST	3.1	2.1	4.0	1.5
Caustic. Eff. (%)	MAN	77.7	76.7	79.18	2.0
	TEST	79.0	77.9	0.1	1.8
TRS	MAN	8.1	4.4	10.3	5.3
(pm)	TEST	7.2	4.5	9.1	4.1

[a] Include all the collected hot-end temperature measurements.
[b] Include only the hot-end temperature measurements that was collected when sawdust has been used as the primary fuel.

In addition to the easily quantifiable energy savings, improvements in the burnt lime quality have also been obtained.[4] Fig. 19 shows the *causticizing efficiency*, which was analyzed five times a week on composite samples, as a function of the production rate. Fig. 20 illustrates the relationship between the *residual calcium carbonate* ($CaCO_3$) content and the production rate. The residual $CaCO_3$ was manually sampled at an 8 h time interval and analyzed with a delay time of about 1–2 hours in the laboratory. While, Fig. 21 shows the causticizing efficiency as a function of the residual $CaCO_3$ content. Despite a slight increase in the residual $CaCO_3$ content of the burnt lime shown in Fig. 20, the causticizing efficiency has been increased by about 1 abs. %. Above-described quality improvements can already be assumed on the basis of the significant reduction shown in the variability and upper quartiles of the hot-end and burning zone temperature measurements (see also Fig. 17 and Table 11).

From the ecological point of the view, the quantifiable major benefit was the decrease in the total reduced sulfur (TRS) emissions. The mean of the TRS emissions, which was measured on-line by an analyzer, was 8.1 ppm in manual operation, and the lower and upper quartiles were 4.4 and 10.3 ppm, respectively. During the testing period, the mean of the TRS emissions was 7.2 ppm, and the lower and upper quartiles were 4.5 and 9.1 ppm, respectively. The mean has been reduced by over 10%, and the upper quartile was reduced by about 12%. A frequency distribution of the TRS emissions collected during manual operation and the testing period are presented in Fig. 22. In addition to the above statistics, Fig. 22 also shows that the proportion of values above 12 ppm, caused predominantly by short-term emission peaks, has been reduced by about 50%. The reduction in the emissions peaks was primarily obtained as a result of

[4] In the laboratory, the quality of the burnt lime is characteristically judged in terms of causticizing efficiency and residual calcium carbonate content (Theliander, 1988). The causticizing efficiency, which usually constitutes from 75% to 80%, is closely correlated to the porosity of the burnt lime and hence also the reactivity of the lime in the slaking. While, the residual carbonate content, which usually constitutes from 1% to 5% of the product, determines the extent of calcination reaction.

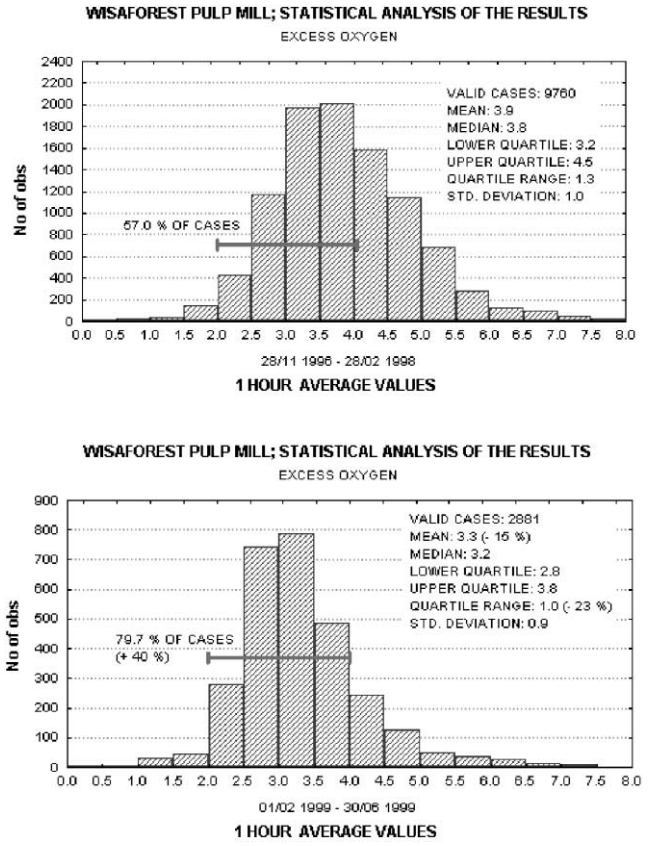

Fig. 16. Frequency distribution of the excess oxygen content during manual operation (above) and the testing period (below).

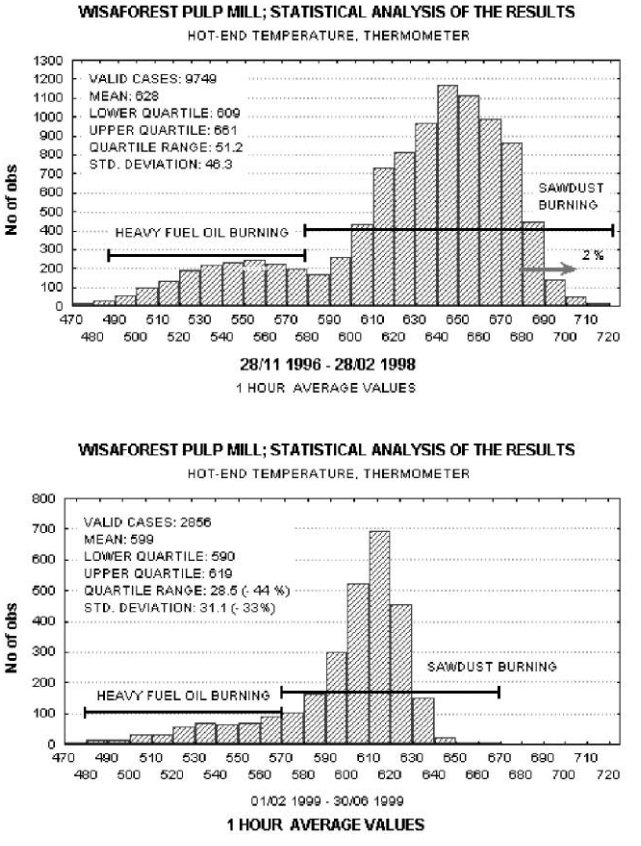

Fig. 17. Frequency distribution of the hot-end temperature during manual operation (above) and the testing period (below).

the improved emission control during high production rate periods, as illustrated in Fig. 23.

Furthermore, the overall balance of *carbon dioxide* (CO_2) *emissions*, which are always formed in organic combustion processes in the presence of oxygen, was positively influenced because fossil fuel, i.e. heavy fuel oil, was replaced by sawmill dust, which is a renewable energy source (see Table 3). In addition, although the CO_2 emissions were not measured during the study period, it can be assumed that the actual CO_2 emissions were also reduced as a result of the overall reduction in the energy consumption. It can also be assumed that *nitrogen oxide* (NO_x) *emissions* were decreased by the reduction in the amount of excess air.

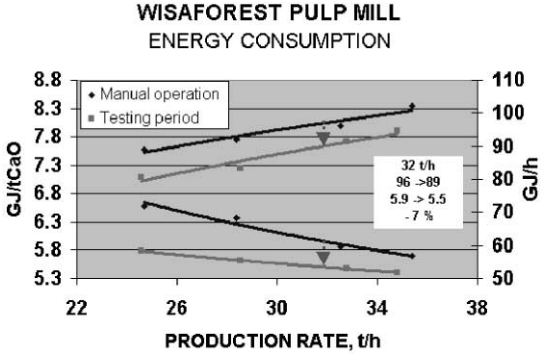

Fig. 18. Energy consumption as a function of the production rate during manual operation and the testing period.

8. Conclusions and future work

The intelligent supervisory-level kiln control system has been successfully operated at the Wisaforest pulp mill in Finland. The major quantifiable benefits was the almost 7% decrease in energy consumption compared to manual operation. In addition, improvements have been obtained in burnt lime quality. From the ecological point of the view, the major quantifiable benefits were an over 10% decrease in the total reduced sulfur (TRS) emissions, and a reduction of about 50% in the proportion of high emission periods. In addition, the testing period of the system has shown an improvement in operational flexibility. Furthermore, the operator's workload has fallen and the plant personnel have a better insight into their process.

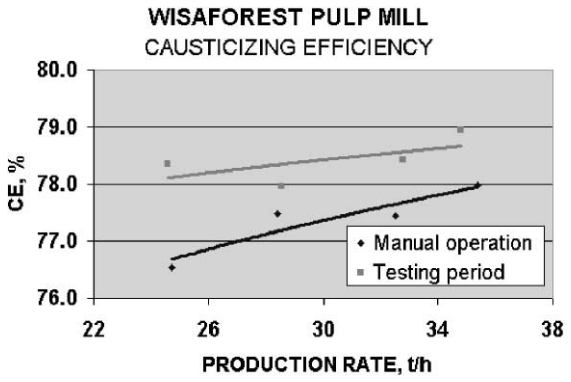

Fig. 19. Causticizing efficiency as a function of the production rate during manual operation and the testing period.

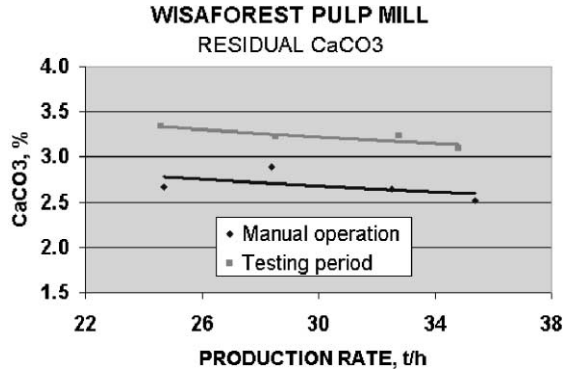

Fig. 20. Residual $CaCO_3$ content as a function of the production rate during manual operation and testing period.

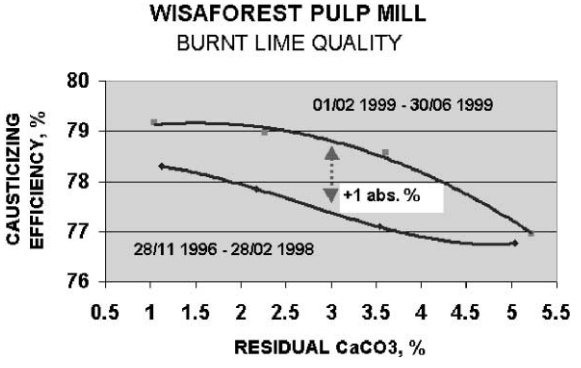

Fig. 21. Causticizing efficiency as a function of the residual $CaCO_3$ content during manual operation (below) and the testing period (above).

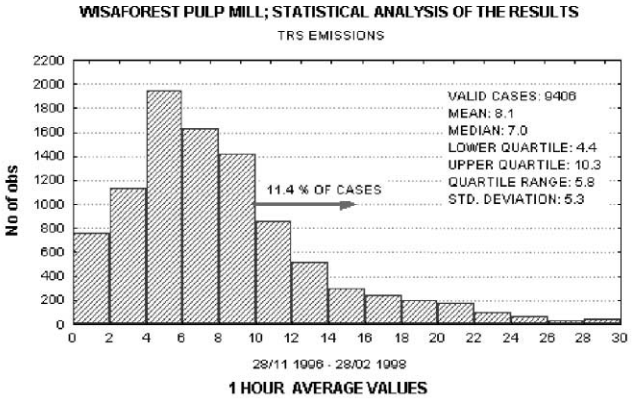

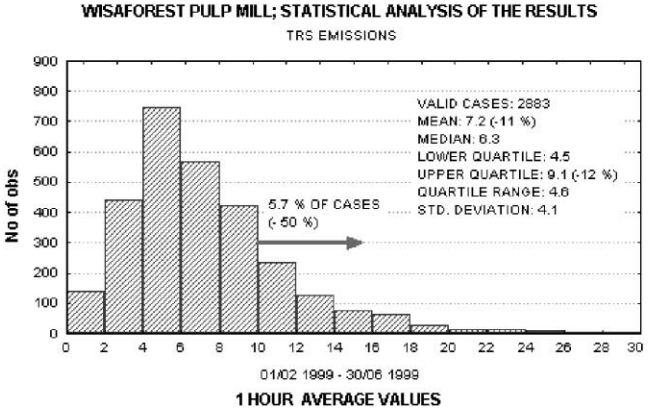

Fig. 22. Frequency distribution of the TRS emissions during manual operation (above) and the testing period (below).

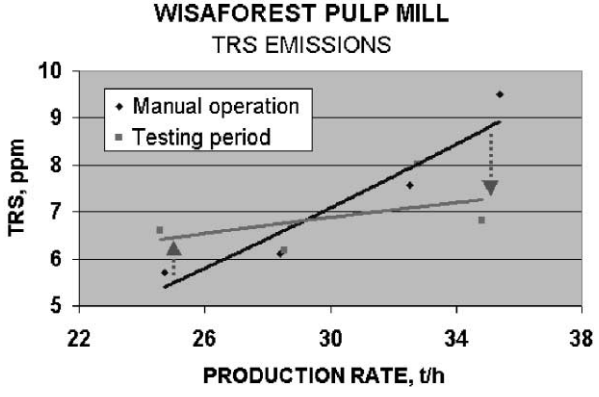

Fig. 23. TRS emissions as a function of the production rate during manual operation and the testing period.

On the other hand, in order to guarantee proper functioning of the system over long-term operation, further development is required in order to enhance maintainability of the implemented system. Furthermore, the kiln operators currently take over operation of the kiln during shutdown, start-up and major plant upsets such as repair of the filter fabric and changes in the fuel mixture. Consequently, an automatic sequence for supervising kiln shutdowns and start-up periods, as well as enhancement of the handling of major disturbances, is recommended as the next step in the development of the system. Improvement in user interface in the form of intelligent alarms and kiln status indications is also recommended.

Of more general relevance, the experience gained during the development of the system has shown that experimental knowledge of a process behavior, together with proper combination of intelligent techniques, can be applied to improve process efficiency and produce considerable benefits. Therefore, the development of a similar type of intelligent system for other industrial processes is also a potential candidate for future developments.

Acknowledgements

This work was supported by UPM-Kymmene and the Academy of Finland. The authors wish to thank the staff of the Wisaforest mill for their valuable support and assistance during this project. An early and shorter version of this paper by the authors, entitled "Intelligent control system of the lime kiln" was presented at IFAC 14th World Congress, Beijing, China, July 1999.

References

Bailey, R. M., & Willison, T. R. (1985). Computerization of the recovery cycle—Lime kiln control and optimization. *Proceedings of the Tappi pulping conference,* Hollywood, USA (pp. 619–627).

Bailey, R. M., & Willison, T. R. (1986). Supervisory control for lime kilns slashes operating costs by up to 20%. *Pulp and Paper*, *60*(2), 100–105.

Barreto, A. G. (1997). Lime kiln hybrid control system. *Proceedings of the IEEE workshop on dynamic modeling control applications for industry*, New York, USA (pp. 44–50).

Brown, K., & Rastogi, L. (1983). Mathematical modeling and computer control of lime kilns. *Proceedings of the Tappi pulping conference*, Atlanta, USA (pp. 585–592).

Charos, G. N., Taylor, R. A., & Arkun, Y. (1991). Model predictive control of an industrial lime kiln. *Tappi Journal*, *74*(2), 203–211.

Crowther, C., Blevins, T., & Burns, D. (1987). A lime kiln control strategy to maximize efficiency and energy management. *Appita Journal*, *40*(1), 29–32.

Dekkiche, E. A. (1991). Advanced kiln control system. *Zement-Kalk-Gips*, *44*(6), 286–290.

Hall, M. B. (1993). Kiln stabilization and control—a COMDALE/C expert system approach. *Proceedings of the 35th IEEE cement industry technical conference*, Toronto, Canada (pp. 201–218).

Hagemoen, S. (1993). An expert system application for lime kiln automation, IEEE, (6), 91–97.

Haspel, D. W., Taylor, R., & Brooks, J. (1991). A new perspective on the cement making process through LINKman. *Proceeding of the cemtech conference*, Praque, Czechoslovakia (pp. 1.3.1–12).

Juuso, E., Ahola, T., & Leiviskä, K. (1996). Fuzzy logic in lime kiln control, *Proceeding of the workshop on tool environments and development methods for intelligent systems*, Oulu, Finland (pp. 111–119).

Juuso, E., Balsa, P., & Valenzuela, L. (1998). Multilevel linguistic equation controller applied to a 1 MW solar power plant. *Proceedings of the 1998 American control conference—ACC'98*, Philadelphia, USA (pp. 3891–3895).

Juuso, E. (1999). Fuzzy control in process industry: The linguistic equation approach. In H. B. Verbruggen, H. -J. Zimmermann, & R. Babuska (Eds.), *Fuzzy Algorithms for Control, International Series in Intelligent Technologies* (pp. 243–300). Kluwer: Boston.

Järvensivu, M., Kivivasara, J., & Saari, K. (1999). A field survey of TRS emissions from a lime kiln. *Pulp and Paper Canada*, *100*(11), 347–350.

Järvensivu, M., Juuso, E., Sievola, H., Leiviskä, K., & Jämsä-Jounela, S. L. (1999). Advanced lime kiln control. *Proceedings of the workshop on tool environments and development methods for intelligent systems*, Oulu, Finland (pp. 94–106).

Järvensivu, M., & Jämsä-Jounela, S. L. (1999). Intelligent control system for the lime kiln. *Proceedings of the 14th IFAC world conference*, Beijing, China (pp. 361–366).

McIlwain, J. A. (1992). Kiln control. *Pulp and Paper Canada*, *93*(11), 34–37.

Nilsson, L. (1997). Skoghall brings cement logic to causticizing. *Pulp and Paper Europe*, *2*(10), 24–27.

Penttinen, R. (1994). Fuzzy control of the lime kiln. M.Sc thesis, Control Engineering Laboratory, University of Oulu (in Finnish).

Ostergaard, J. (1993). Fuzzy control of cement kilns: a retrospective summary. *Proceedings of the first European congress on fuzzy and intelligent technologies*, Aachen, Germany.

Ribeiro, B. M., & Correia, A. D. (1995). Lime kiln simulation and control by neural networks, *Neural networks for chemical engineers* (pp. 163–191). Amsterdam: Elsevier Science Ltd.

Ruotsalainen, J. (1994). *Control of the pulp mill chemical recovery circuit*. Thesis for licentiate in technology, Control Engineering Laboratory, University of Oulu.

Scheuer, A., & Principato, M. (1995). Experience with the PYROEXPERT kiln control system at the Leimen cement. *ZKG International*, *48*(9), 464–471.

Sievola, H. (1999). *Hot end temperature control of a lime kiln based on linguistic equations*. M. Sc. thesis, Control Engineering Laboratory, University of Oulu (in Finnish).

Smith, D. B., & Edwards, L. (1991). Dynamic mathematical model of a rotary lime kiln. *Proceedings of the TAPPI engineering conference*, Atlanta, USA (pp. 447–455).

Smith, D. B., & Aggarwal, P. (1998). Advanced lime kiln control: Operating results from a mill installation. *Proceedings of the Tappi Process Control, Electrical & Information Conference*, Atlanta, USA (pp. 347–353).

Sutinen, R. (1981). Causticizing plant and lime kiln computer control. *Pulp and Paper Canada*, *82*(8), 90–95.

Theliander, H. (1988). A system analysis of the chemical recovery plant of the sulfate pulping process. *Nordic Pulp and Paper Research Journal*, *3*(2), 60–67.

Uronen, P., & Aurasmaa, H. (1979). Modelling and simulation of causticization plant and lime kiln. *Pulp and Paper Canada*, *80*(6), T162–T165.

Uronen, P., & Leiviskä, K. (1989). New topics in lime kiln control. *Pulp and Paper Canada*, *90*(9), 113–117.

Valiquette, J. (1999). Practical aspects of model-predictive control implementation on an industrial lime kiln. *Tappi Journal*, *82*(5), 130–136.

Yang, B., Yi, L., & Shouning, Q. (1997). A rule based cement kiln control system using neural networks. Proceeding *on IEEE international conference on intelligent processing systems*, vol. 1, Beijing, China (pp. 493–497).

Zanovello, R., & Budman, H. (1999). Model predictive control with soft constraints with application to lime kiln control. *Computers and Chemical Engineering*, *23*(6), 791–806.